JACS
JOURNAL OF THE AMERICAN CHEMICAL SOCIETY
Article
pubs.acs.org/JACS

Isolation of Three Isomers of Sm@C_{84} and X-ray Crystallographic Characterization of Sm@D_{3d}(19)-C_{84} and Sm@C_2(13)-C_{84}

Hua Yang,[†,‡] Meilan Yu,[§,‡] Hongxiao Jin,[†] Ziyang Liu,*[,§,†] Mingguang Yao,[∥] Bingbing Liu,[∥] Marilyn M. Olmstead,*[,⊥] and Alan L. Balch*[,⊥]

[§]College of Life Science, Zhejiang Sci-Tech University, Hangzhou 310018, China
[†]College of Materials Science and Engineering, China Jiliang University, Hangzhou 310018, China
[∥]National Laboratory of Superhard Materials, Jilin University, Changchun 130012, China
[⊥]Department of Chemistry, University of California, One Shields Avenue, Davis, California 95616, United States

Supporting Information

ABSTRACT: Three isomers with the composition Sm@C_{84} were isolated from carbon soot obtained by electric arc vaporization of carbon rods doped with Sm_2O_3. These isomers were labeled Sm@C_{84}(I), Sm@C_{84}(II), and Sm@C_{84}(III) in order of their elution times during chromatography on a Buckyprep column with toluene as the eluent. Analysis of the structures by single-crystal X-ray diffraction on cocrystals formed with Ni^{II}(octaethylporphyrin) reveals the identities of two of the isomers: Sm@C_{84}(I) is Sm@C_2(13)-C_{84}, and Sm@C_{84}(III) is Sm@ D_{3d}(19)-C_{84}. Sm@C_{84}(II) can be identified as Sm@C_2(11)-C_{84} on the basis of the similarity of its UV/vis/NIR spectrum with that of Yb@C_2(11)-C_{84}, whose carbon cage has been characterized by ^{13}C NMR spectroscopy. Comparison of the three Sm@C_{84} isomers identified in this project with two prior reports of the preparation and isolation of isomers of Sm@C_{84} indicate that five different Sm@C_{84} isomers have been found and that the source of samarium used for the generation of fullerene soot is important in determining which of these isomers form.

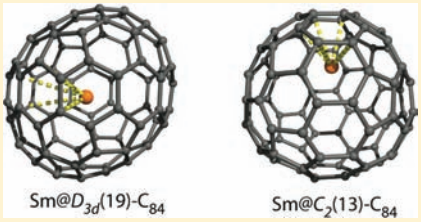

INTRODUCTION

Filling the void at the center of a fullerene cage has resulted in the formation of an impressive array of endohedral fullerenes ever since Heath et al.[1] reported the mass spectroscopic detection of LaC_{60} and La_2C_{60}.[2,3] Thus, molecules such as dihydrogen[4] and water[5] and have been inserted into the C_{60} cage, while large clusters like $Sc_4(\mu\text{-}O)_2$ and $Sc_4(\mu\text{-}O)_3$[6] have been trapped inside the I_h-C_{80} cage. However, the simplest endohedral fullerenes contain only a single atom. That single atom may be a relatively unreactive noble gas atom or it may be an electropositive metal atom that transfers electrons onto the π-orbitals of the fullerene cage. The properties of these endohedral fullerenes can be altered by varying the atoms contained inside. As a result, endohedral fullerenes containing gadolinium atoms have magnetic properties that make them useful in magnetic resonance imaging (MRI),[7,8] and endohedrals containing radioactive metals may be useful in nuclear medicine.[9]

In endohedral fullerenes containing electropositive metals like the lanthanides, eletrons are transferred between the metal and the cage, and a zwitterionic structure, $M^{x+}@(C_{2n})^{x-}$, results.[10,11] With Sc, Y, La, Ce, Pr, Nd, Gd, Tb, Dy, Ho, Er, and Lu, the metals adopt their usual 3+ state and three electrons are transferred to the cage. However, with endohedral fullerenes involving samarium (as well as Eu, Tm, Yb, and the alkaline earth metals), only two electrons are transferred to the cage.

More than 25 fullerenes with the composition Sm@C_{2n} and cage sizes ranging from C_{74} to C_{96} have been isolated, but little is known about the structures of these compounds.[12,13] Electron energy-loss spectroscopic (EELS) measurements have shown that the oxidation state of the samarium is 2+ in some of the smaller cages.[14,15] In order to further characterize the Sm@C_{2n} family of compounds, we have begun a series of studies to determine the structures of its members through single-crystal X-ray diffraction. Recently, we reported structural studies on four isomers of Sm@C_{90}, the most extensive series of isomers of any individual endohedral fullerene to be examined by X-ray diffraction. That work determined the structures of Sm@C_2(40)-C_{90}, Sm@C_2(42)-C_{90}, Sm@C_{2v}(46)-C_{90}, and Sm@C_2(45)-C_{90}.[16] Interestingly, the cages of these four isomers can be related pairwise to one another through a sequential series of Stone–Wales transformations.[17] Here, we report the isolation of three isomers of Sm@C_{84} and the crystallographic characterization of two of these.

For fullerenes larger than C_{70}, the cage can exist in different isomeric forms and the number of isomers increases as the number of carbon atoms in the fullerene increases.[18] For C_{84} there are 24 isomers that obey the isolated pentagon rule (IPR), which requires that each of the twelve pentagons of a fullerene is surrounded by five hexagons.[18] Early ^{13}C NMR studies have shown that the major soluble isomers of C_{84} that form in the electric arc synthesis of fullerenes are a D_2-C_{84} isomer [subsequently identified as D_2(22)-C_{84}] and the

Received: December 17, 2011
Published: February 14, 2012

   dx.doi.org/10.1021/ja211785u | J. Am. Chem. Soc. 2012, 134, 5331–5338

$D_{2d}(23)$-C_{84} isomer, which are present in a 2:1 abundance ratio.[19] Since then a plethora of empty-cage C_{84} isomers have been isolated or detected. Thus, Dennis et al.[20] isolated seven isomers C_{84} and determined their symmetry by ^{13}C NMR spectroscopy. In addition to the major isomers, $D_2(22)$-C_{84} and $D_{2d}(23)$-C_{84}, they identified five minor isomers as having C_2, C_s(a), C_s(b), D_{2d}(I), and D_2(II) symmetry. Alteration of the synthesis process through doping of the carbon rods can produce other C_{84} isomers. For example, Tagmatarchis et al.[21] found that gadolinium-doped carbon rods produced a mixture of the D_{6h} and D_{3d} isomers of C_{84} as determined by ^{13}C NMR spectroscopy. Similarly, carbon rods doped with Dy_2O_3 produced a new C_2 isomer of C_{84}, whose symmetry was again identified by ^{13}C NMR spectroscopy .[22]

Three-dimensional characterization of C_{84} cages began with crystallization and X-ray diffraction work on η^2-($D_{2d}(23)$-C_{84})Ir(CO)Cl[P(C_6H_5)$_3$]$_2$.[23] That study also demonstrated the close structural similarity of $D_2(22)$-C_{84} and $D_{2d}(23)$-C_{84}, since a small amount of the $D_2(22)$-C_{84} isomer was also found in the crystal. $D_2(22)$-C_{84} and $D_{2d}(23)$-C_{84} are related by a single Stone–Wales transformation.[17] A combined crystallographic and ^{13}C NMR study has shown that C_s(b), initially isolated by Dennis et al., is $C_s(14)$-C_{84}.[24] Treatment of mixtures of higher fullerenes with CF_3I or C_2F_5I, followed by chromatographic separation and crystallization, has led to the identification of the following C_{84} cage isomers in the resulting perfluoroalkyl adducts: $C_2(11)$,[25] $D_{2d}(23)$,[26] $D_2(4)$,[26] $D_2(23)$,[26] $C_{2v}(18)$,[26] and $C_s(16)$.[26] Curiously, the first endohedral fullerenes containing the C_{84} cage that have been crystallographically characterized were the series of non-IPR endohedrals M_3N@$C_s(51365)$-C_{84} (M = Tb, Gd, or Tm).[27,28] While this paper was under review, crystallographic characterization of the IPR-obeying Sc_2C_2@$D_{2d}(23)$-C_{84} was reported.[29]

RESULTS

Isolation of Three Isomers of Sm@C_{84}. Carbon soot containing samarium endohedral fullerenes along with empty-cage fullerenes was obtained by vaporizing a graphite rod filled with Sm_2O_3 and graphite powder in an electric arc as outlined earlier.[17,30,31] This carbon soot was extracted with *o*-dichlorobenzene, and the soluble extract was subjected to a multistage high-pressure liquid chromatographic (HPLC) isolation process involving two complementary chromatographic columns (Buckyprep-M and Buckyprep) with either chlorobenzene or toluene as the eluent. Three isomers of Sm@C_{84} were isolated. Figure 1 shows the HPLC chromatograms of the purified samples of the Sm@C_{84} isomers we obtained.

Figure 2 shows the laser-desorption ionization time-of-flight (LDI-TOF) mass spectrum of Sm@C_{84}(I) along with the spectrum computed from isotope abundances. The corresponding spectra (see Supporting Information) for the other two isomers are nearly identical. The UV–vis–NIR absorption spectra of the individual isomers are shown in Figure 3. Sm@C_{84}(II) has the lowest energy absorptions with bands occurring at 1580, 1296, 1107, 855, and 737 nm. The spectrum of Sm@C_{84}(III) consists of four major absorptions at 1073, 925, 827, and 726 nm, while the spectrum of Sm@C_{84}(I) shows absorptions at 1117, 1026, 968, 818sh, 780, 646, and 596 nm.

Identification of Sm@C_{84}(III) as Sm@D_{3d}(19)-C_{84}. Since this isomer has higher symmetry and fewer structural complications, we will discuss it first. To facilitate the formation of sufficiently ordered crystals for X-ray diffraction,[32] the endohedral fullerene was cocrystallized with

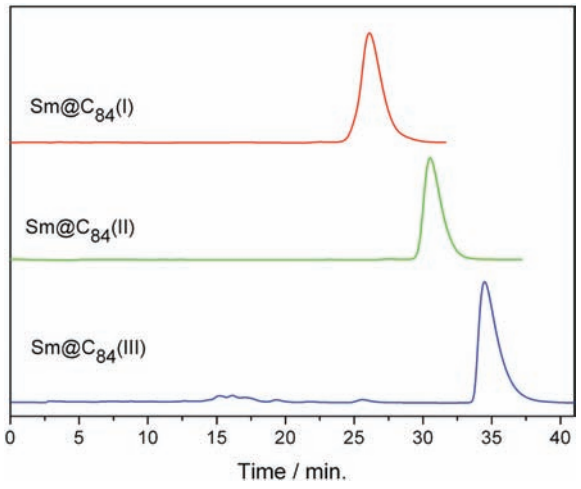

Figure 1. Chromatograms of the isolated Sm@C_{84} isomers on a Buckyprep column with toluene as the eluent. The HPLC conditions were flow rate 4.0 mL/min and detection wavelength 450 nm.

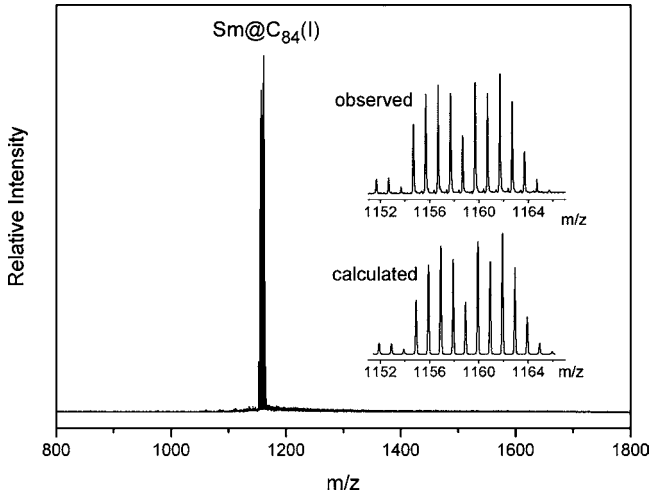

Figure 2. LDI-TOF mass spectra of the purified sample of Sm@C_{84}(I). (Insets) Expansions of experimental and theoretical isotope distributions. The very similar, experimental mass spectra of the other two isomers appear in the Supporting Information.

Ni^{II}(octaethylporphyrin) [Ni^{II}(OEP)] in toluene solution to form black crystals of Sm@D_{3d}(19)-C_{84}·Ni^{II}(OEP)·2(toluene). Figure 4 shows the structure of the $D_{3d}(19)$-C_{84} cage alone with the 3-fold axis aligned vertically. As the figure shows, this 3-fold axis passes through the hexagons at opposite poles of the molecule. The distance between the centroids of these hexagons is 8.519 Å. There are three perpendicular 2-fold axes that also pass through centers of hexagons, with centroid-to-centroid distances of 7.611, 7.638, and 7.645 Å.

Figure 5 shows the relative orientations of the Sm@$D_{3d}(19)$-C_{84} and Ni^{II}(OEP) molecules in Sm@$D_{3d}(19)$-C_{84}·Ni^{II}(OEP)·2(toluene). As outlined in the Experimental Section, there are two orientations of the C_{84} cage that are related by a crystallographic mirror plane and occupy a common site. Only one of these orientations is shown in Figure 5. Inside this cage, however, we show the two major positions of the samarium atom, each with 0.40 fractional occupancy. Sm1A is generated by reflection of Sm1 through a crystallographic mirror plane that, unfortunately, does not coincide with any of the mirror planes in the C_{84} cage. As the drawing shows,

dx.doi.org/10.1021/ja211785u | J. Am. Chem. Soc. 2012, 134, 5331–5338

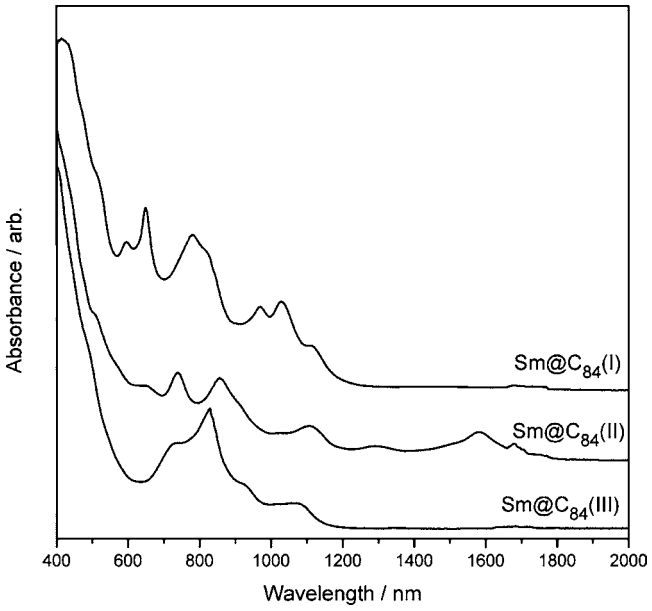

Figure 3. UV−vis−NIR absorption spectra of the purified isomers of Sm@C_{84} in carbon disulfide solution. The small absorbances in the 1650−1800 nm range are solvent artifacts.

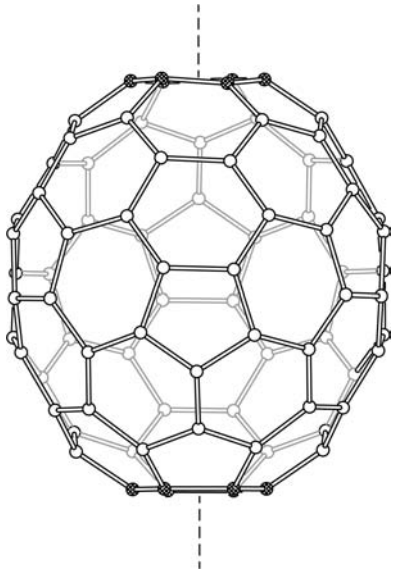

Figure 4. Drawing showing the D_{3d}(19)-C_{84} carbon cage in Sm@D_{3d}(19)-C_{84}·Ni^{II}(OEP)·2(toluene). The 3-fold axis is aligned vertically. For clarity, the positioning of the internal samarium atom is not shown.

Sm1 is positioned nearest a hexagon (shown in green) on the interior of the fullerene, while Sm1A is near a pentagon, which is highlighted in red. In the other, equivalent location of the fullerene cage, these orientations are reversed: Sm1 is near a pentagon and Sm1A is beside a hexagon. Due to the similarity in Sm···C distances and the ambiguity created by the crystallographic symmetry, there is no way to determine whether there is any preference for one or the other location of the metal atom. Figure 6 shows the two likely locations of the samarium atoms and their distances from the neighboring carbon atoms.

Identification of Sm@C_{84}(I) as Sm@C_2(13)-C_{84}. Black crystals of Sm@C_2(13)-C_{84}·Ni^{II}(OEP)·2(toluene) were obtained by mixing solutions of Sm@C_{84}(I) and Ni^{II}(OEP) in toluene and were used for the structure determination. Figure 7 shows a drawing of the C_2(13)-C_{84} cage alone without the encapsulated samarium atom. As the figure shows, the 2-fold axis runs through the centers of the hexagons at the top and bottom of the picture. The distance between the centroids of these hexagons is 7.860 Å, which is considerably shorter than the comparable distance (8.519 Å) along the principal axis of D_{3d}(19)-C_{84}.

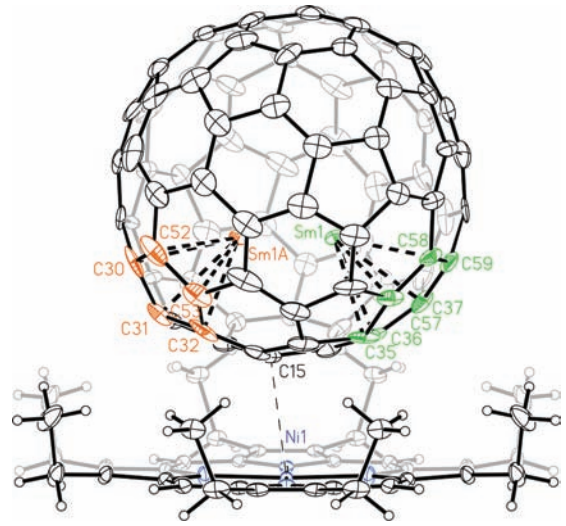

Figure 5. Drawing showing the interaction between the fullerene and porphyrin in Sm@D_{3d}(19)-C_{84}·Ni^{II}(OEP)·2(toluene) with 30% thermal ellipsoids. Only one orientation of the fullerene cage is shown. While the cage contains only a single samarium atom, the drawing shows the major samarium site, Sm1, with 0.40 fractional occupancy and its symmetry-generated counterpart, Sm1A. Carbon atoms nearest to site Sm1 are shown in green; those atoms closest to Sm1A are shown in red. For clarity, the toluene molecules are not shown. The vertically aligned crystallographic mirror plane bisects Ni1 and lies perpendicular to the plane of the page.

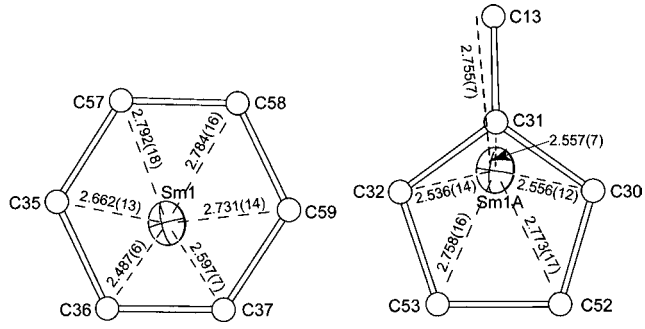

Figure 6. Drawing showing the positioning of the principal samarium sites with 0.40 occupancy with the adjoining carbon atoms of the fullerene cage for Sm@D_{3d}(19)-C_{84}·Ni^{II}(OEP)·2(toluene).

Figure 8 shows the relative orientations of the Sm@C_2(13)-C_{84} and Ni^{II}(OEP) molecules in Sm@C_2(13)-C_{84}·Ni^{II}(OEP)·2-(toluene). Two major orientations of the C_2(13)-C_{84} cage with fractional occupancy of 0.4629(15) are situated at a common site. One of these orientations is shown in Figure 8. Additionally, there are two locations of a minor form of the same cage that overlap with the major site. Neither of these minor orientations is shown in Figure 8. Within these cages, there are 10 sites for the samarium atoms along with another 10 generated by the crystallographic mirror plane. The major site

dx.doi.org/10.1021/ja211785u | J. Am. Chem. Soc. 2012, 134, 5331−5338

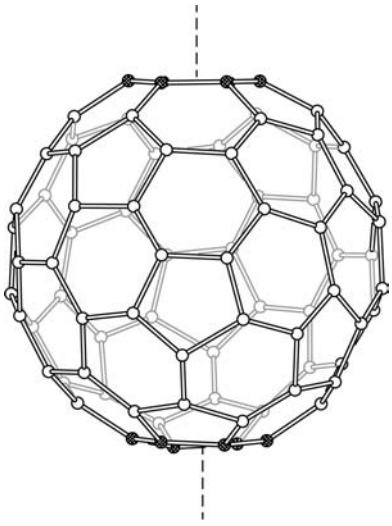

Figure 7. Drawing showing the $C_2(13)$-C_{84} carbon cage in Sm@$C_2(13)$-C_{84}·Ni^{II}(OEP)·2(toluene). The 2-fold axis is aligned vertically. For clarity, the positioning of the internal samarium atom is not shown.

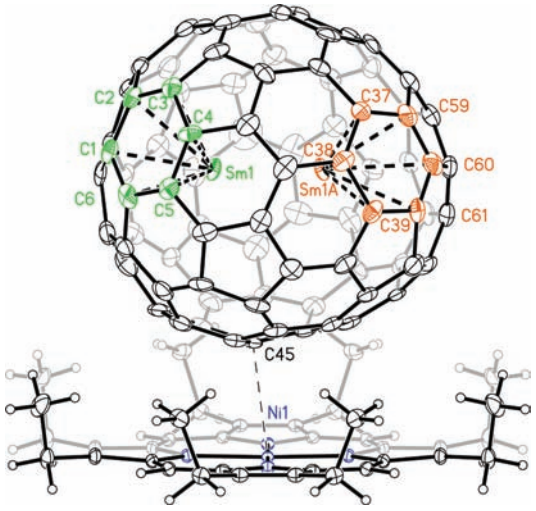

Figure 8. Drawing showing the interaction between the fullerene and porphyrin in Sm@$C_2(13)$-C_{84}·Ni^{II}(OEP)·2(toluene) with 30% thermal ellipsoids. Only one orientation of the fullerene cage is shown. While the cage contains only a single samarium atom, the drawing shows the major samarium site, Sm1, with 0.21 fractional occupancy and its symmetry-generated counterpart, Sm1A. The other, more minor samarium atoms sites are not shown. Carbon atoms nearest to site Sm1 are shown in green; those atoms closest to Sm1A are shown in red. For clarity, the toluene molecules are not shown. The vertically aligned crystallographic mirror plane bisects Ni1 and lies perpendicular to the plane of the page.

has a fractional occupancy of 0.21, while the minor ones have occupancies in the 0.05–0.02 range. Figure 9 shows the location of the major site, Sm1, and the corresponding symmetry-generated site, Sm1A. Sm1 and Sm1A are located beneath the centers of hexagons on the fullerene inner surface. Figure 9 shows the distances from the two major samarium sites to the nearby cage carbon atoms.

Computational Studies of the Relative Stabilities of the Sm@C_{84} Isomers. To provide insight into the electronic and geometric structures of the Sm@C_{84} isomers, geometric optimizations via DFT methodology were conducted for Sm@

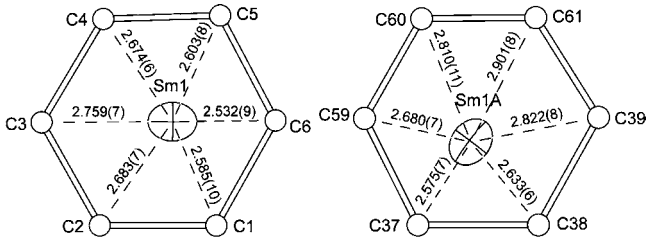

Figure 9. Drawing showing the positioning of the principal samarium sites with 0.21 occupancy with the adjoining carbon atoms of the fullerene cage for Sm@$C_2(13)$-C_{84}·Ni^{II}(OEP)·2(toluene).

$D_{3d}(19)$-C_{84}, and three other isomers: Sm@$C_2(13)$-C_{84}, Sm@$C_1(12)$-C_{84}, and Sm@$C_2(11)$-C_{84}. These three particular cages were investigated because their counterparts with ytterbium have been identified through ^{13}C NMR measurements and DFT calculations. A vibrational analysis was also performed to confirm that the optimized geometries are all discrete energy minima. The results are shown in Table 1. Among these four

Table 1. Relative Energies and HOMO–LUMO Gaps of Sm@C_{84} Isomers Calculated at B3LYP/3-21g (CEP-31g for Sm) Level

isomer	ΔE, kcal·mol^{-1}	HOMO–LUMO gap, eV
Sm@$C_2(13)$-C_{84}	0.0000	1.837
Sm@$C_1(12)$-C_{84}	2.7480	1.373
Sm@$D_{3d}(19)$-C_{84}	4.4102	1.843
Sm@$C_2(11)$-C_{84}	14.2054	1.386

endohedrals, Sm@$C_2(13)$-C_{84} is the most stable. Experimentally, it is also the most abundant of the isomers detected in this study. On the other hand, Sm@$D_{3d}(19)$-C_{84} has the largest computed HOMO–LUMO gap.

Because the electronic distribution for samarium- and ytterbium-containing endohedral fullerenes can be represented by an ionic model, $M^{2+}@(C_{2n})^{2-}$ (M = Sm or Yb), where the cage acquires two electrons from the interior metal atom, calculations were also performed to determine the relative stabilities of the dianions of all of the 24 IPR isomers of C_{84}. Those relative stabilities are listed in Table SI-1 (see Supporting Information). The dianion of $D_{3d}(19)$-C_{84} has both the greatest stability and the largest HOMO–LUMO gap among the 24 non-IPR cages, conditions which are favorable for the formation of this isomer. Figure 10 shows the molecular orbital energies computed for the neutral, di-, tri-, and tetra-anionic forms of the empty cage $D_{3d}(19)$-C_{84} via DFT methodology. The neutral cage has a moderate HOMO–LUMO gap of 1.38 eV. In addition, the calculated relative energy for this neutral cage (see Supporting Information, Table SI-2) was comparable to those of the corresponding isomers of empty C_{84} isolated and characterized by NMR.[20] The gap increases to 1.76 eV when two electrons are introduced into the a_{1g} orbital of the neutral $D_{3d}(19)$-C_{84}, while it narrows to only 0.65 or 0.66 eV when another two additional electrons are added sequentially to produce the trianion with a doublet state and the tetra-anion with a triplet ground state. Figure 11 shows the corresponding molecular orbital energies computed for the neutral, di-, tri-, and tetra-anionic forms of the empty cage $C_2(13)$-C_{84}. Again, the HOMO–LUMO gaps increase upon addition of two electrons to form the diamagnetic dianion and

dx.doi.org/10.1021/ja211785u | J. Am. Chem. Soc. 2012, 134, 5331–5338

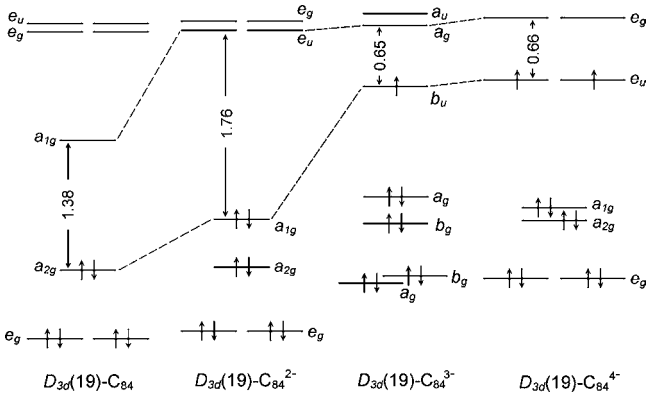

Figure 10. Molecular orbital energy levels (in electronvolts) for the neutral form as well as di-, tri-, and tetra-anions of the empty $D_{3d}(19)$-C_{84} molecule. The calculations were conducted at B3LYP/6-31G(d) level. For the trianion, a Jahn–Teller distortion lowers the symmetry to C_{2h}, and the labels in the figure reflect this symmetry lowering.

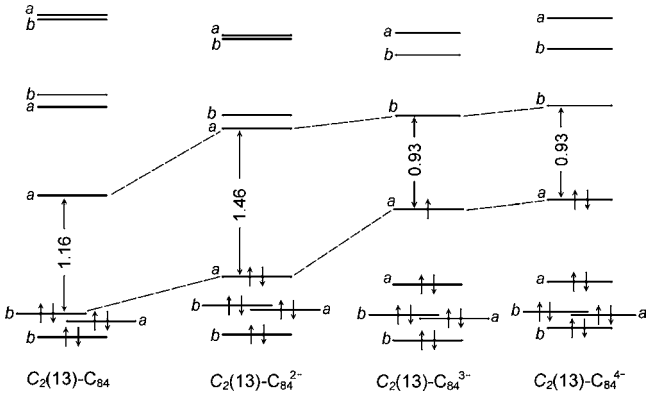

Figure 11. Molecular orbital energy levels (in electronvolts) of the neutral form as well as di-, tri-, and tetra-anions of the empty $C_2(13)$-C_{84} molecule. The calculations were conducted at B3LYP/6-31G(d) level.

then decrease when one or two more electrons are added to produce the trianion and the tetra-anion.

DISCUSSION

This work has produced the first detailed structural characterization of endohedral fullerenes with the C_{84} cage: Sm@$C_2(13)$-C_{84} and Sm@$D_{3d}(19)$-C_{84}. Structural studies of endohedral fullerenes that utilize the C_{84} cage are relatively rare. Oddly, the first three examples of C_{84} endohedrals to be examined by X-ray diffraction, $M_3N@C_s(51365)$-C_{84} (M = Tb, Gd, or Tm), utilized a non-IPR cage that has a single pair of abutting pentagons. In contrast, both $C_2(13)$-C_{84} and $D_{3d}(19)$-C_{84} obey the IPR. Considerable attention has also been given to the characterization of the novel carbide, $(Sc_2C_2)@D_{2d}(23)$-C_{84}, whose identity has been established through several ^{13}C NMR studies and a recent crystallographic report.[29,33,34]

Table 2 summarizes the comparative UV–vis-NIR absorption data for the various Sm@C_{84} isomers that have been reported and also notes the relationship of the absorption spectra of these endohedrals with those of the isomers of Ca@C_{84}[35] and Yb@C_{84} (vide infra).[36] The compounds with similar UV–vis–NIR spectra are arranged into vertical columns, while the rows represent the isomers found by different laboratories, as noted in the references. Previously, Okazaki et al.[12] reported the isolation of three isomers of Sm@C_{84} (which we label I^O, II^O, and III^O). Additionally, J. Liu et al.[13] reported the isolation of three isomers of Sm@C_{84} (here labeled I^L, II^L, and III^L). However, comparison of the UV–vis–NIR absorption of these isomers indicates that each of the three research groups isolated a different set of isomers of Sm@C_{84}. The UV–vis–NIR spectrum of Sm@C_{84}(I) shown in Figure 3 matches the spectra reported for Sm@$C_{84}(I^L)$, and for Sm@$C_{84}(I^O)$. Thus, the initially eluting isomer found by all three groups is the same. However, the spectrum we report for Sm@C_{84}(II) does not match any of the other spectra reported by Liu et al. but does match the spectrum reported by Okazaki et al. for their last eluting isomer, Sm@$C_{84}(III^O)$. The spectrum shown in Figure 3 for Sm@C_{84}(III) is unlike any of the spectra reported by Liu et al. or by Okazaki et al. Thus, Sm@C_{84}(III) is a new isomer. Finally, the absorption spectra of the second eluting isomers Sm@$C_{84}(II^L)$ and Sm@$C_{84}(II^O)$ are similar, but an isomer with a corresponding spectrum was not encountered in our work. All in all, five isomers of Sm@C_{84} have been observed, although we isolated only three of these. Two of these three isomers have been obtained in a form that led to structural characterization through X-ray diffraction.

The variations in the Sm@C_{84} isomers obtained by the three different laboratories can be traced to differences in the preparative procedures, particularly the source of the samarium. In our laboratory, the graphite rods used for fullerene generation were doped with Sm_2O_3. However, Okazaki et al.[12] used a mixture of graphite powder, silicon carbide and Sm_2Co_{17} alloy as their samarium source, while Liu et al.[13] used $SmNi_2$ alloy mixed with graphite powder as their samarium source. Thus, the set of Sm@C_{84} isomers that are produced is not the set of thermodynamically most stable isomers but is controlled by various compounds present during the arcing process. Other reports have also noted the effects of various additives on the yields of fullerene isomers produced.[21,22]

In addition to characterization of the Sm@C_{84} isomers, the data in Table 2 allow some comparisons to be drawn concerning related ytterbium- and calcium-containing endohedral fullerenes. The structures of the cages for three isomers of

Table 2. Classification of the Structures of M@C_{84} Isomers on the Basis of Similarities of UV–Vis–NIR Spectra

	cage symmetry					
ref	unknown A	$C_2(13)$-C_{84}	$C_1(12)$-C_{84}	$C_2(11)$-C_{84}	$D_{3d}(19)$-C_{84}	unknown F
this work		Sm@C_{84}(I)[a]		Sm@C_{84}(II)	Sm@C_{84}(III)[a]	
13		Sm@$C_{84}(I^L)$	Sm@$C_{84}(II^L)$			Sm@$C_{84}(III^L)$
12		Sm@$C_{84}(I^O)$	Sm@$C_{84}(II^O)$	Sm@$C_{84}(III^O)$		
36,41	Yb@C_{84}(I)	Yb@C_{84}(II)[b]	Yb@C_{84}(III)[b]	Yb@C_{84}(IV)[b]		
35		Ca@C_{84}(I)	Ca@C_{84}(II)			

[a]Structure determined by single-crystal X-ray diffraction, this work. [b]Structure determined by ^{13}C NMR spectroscopy; see ref 36 above.

dx.doi.org/10.1021/ja211785u | J. Am. Chem. Soc. 2012, 134, 5331–5338

Yb@C_{84} have been determined through ^{13}C NMR spectroscopy on ^{13}C-enriched samples and comparisons of these experimental spectra with computed spectra.[35] It is gratifying to note that our crystallographic results for Sm@C_{84}(I) and the ^{13}C NMR spectroscopic results for Yb@C_{84}(II) agree that these two endohedrals utilize the same $C_2(13)$-C_{84} cage, since both compounds have similar UV−vis−NIR spectra. On the basis of the UV−vis−NIR spectral comparison, Ca@C_{84}(I) also uses the $C_2(13)$-C_{84} cage. Our Sm@C_{84}(II), which has a UV−vis−NIR spectrum similar to that of Yb@C_{84}(IV), is highly likely to utilize the $C_2(11)$-C_{84} cage.

While our studies have definitively identified the fullerene cage isomers involved with these isomers of Sm@C_{84}, there is uncertainty in the location of the samarium ions, which display considerable disorder, inside the cages. This situation may indicate that the samarium ions are relatively free to move about inside the cage and may reflect the weaker interaction of a 2+ metal ion with a dianionic cage rather than a 3+ metal ion with a trianionic cage. A similar degree of uncertainty was also found in the positions of the samarium ions in the four isomers of Sm@C_{90} that have been crystallographically characterized.[16]

As noted previously, the four isomers of Sm@C_{90} that have been isolated are related to one another in pairwise fashion through a series of Stone−Wales transformations.[17] Five isomers of Sm@C_{84} are now known, and the structures of four of these [Sm@$C_2(13)$-C_{84}, Sm@$C_1(12)$-C_{84}, Sm@$C_2(11)$-C_{84}, and Sm@$D_{3d}(19)$-C_{84}] can be inferred from the data given in Table 2. However, unlike the situation for Sm@C_{90}, where all four isomers were obtained from a single method of fullerene generation, the five isomers of Sm@C_{84} have been obtained by three different routes, each of which produced evidence for only three isomers. Of course minor amounts of other isomers could have been present in any of these preparations. For these Sm@C_{84} isomers, a single Stone−Wales transformation interconverts Sm@$C_2(13)$-C_{84} and Sm@$C_1(12)$-C_{84}. Likewise, Sm@$C_1(12)$-C_{84} and Sm@$C_2(11)$-C_{84} are related by another Stone−Wales transformation. However, Sm@$D_{3d}(19)$-C_{84} cannot be converted into any of the other three isomers by a single Stone−Wales transformation, but it can be related to these other isomers through a series of transformations involving as yet unobserved isomers.

CONCLUSIONS

Five different Sm@C_{84} isomers have been identified in three different studies. This aricle reports definitive X-ray crystallographic characterization of two of these isomers, Sm@$D_{3d}(19)$-C_{84} and Sm@$C_2(13)$-C_{84}. Two other isomers can be identified as Sm@$C_1(12)$-C_{84} and Sm@$C_2(11)$-C_{84} on the basis of spectral similarlities to corresponding yterbium endohedral fullerenes, whose structures have been determined by ^{13}C NMR spectroscopy. The structure of the fifth Sm@C_{84} isomer remains unknown. The source of samarium used for the generation of fullerene soot appears to be important in determining which of these isomers form.

EXPERIMENTAL SECTION

Formation and Isolation of the Sm@C_{84} Isomers. An 8 × 150 mm graphite rod filled with Sm_2O_3 and graphite powder (Sm:C atomic ratio 1:40) was vaporized as the anode in direct current(dc)arc discharge under optimized conditions. The raw soot was sonicated in *o*-dichlorobenzene for 8 h and then filtered with aid of vacuum. After removal of the solvent with a rotary evaporator, chlorobenzene was added to redissolve the dry extract. The resulting solution was subjected to a four-stage HPLC isolation process without recycling. Chromatographic details are given in the Supporting Information.

The purity and composition of the samples of isomers of Sm@C_{84} were verified by laser desorption ionization time-of-flight mass spectrometry (LDI-TOF MS). Ultraviolet−visible−near-infrared (UV−vis−NIR) spectra were obtained through the use of a UV-4100 spectrophotometer (Hitachi High-Technologies Corp.) with samples dissolved in carbon disulfide.

Crystal Growth. Black crystals of Sm@$C_2(13)$-C_{84}·Ni^{II}(OEP)·2-(toluene) were obtained by slow diffusion of solutions of Sm@C_{84}(I) dissolved in toluene and of Ni^{II}(OEP) also in toluene. Crystals of Sm@$D_{3d}(19)$-C_{84}·Ni^{II}(OEP)·2(toluene) were obtained in a similar fashion from a purified sample of Sm@C_{84}(III).

Crystal Structure Determinations. The black crystals of both cocrystals were mounted in the nitrogen cold stream provided by a Cryo Industries low-temperature apparatus on the goniometer head of a Bruker SMART diffractometer equipped with an ApexII CCD detector. Data were collected with the use of Mo Kα radiation (λ = 0.710 73 Å). Crystal data are given in Table 3. The structures were solved by direct methods (SHELXS97) and refined by full-matrix least-squares on F^2 (SHELXL97).[37]

Table 3. Crystal Data and Data Collection Parameters

	Sm@$C_2(13)$-C_{84} ·Ni^{II}(OEP)·2(toluene)	Sm@$D_{3d}(19)$-C_{84} ·Ni^{II}(OEP)·2(toluene)
isomer	Sm@C_{84}(I)	Sm@C_{84}(III)
formula	$C_{134}H_{60}N_4NiSm$	$C_{134}H_{60}N_4NiSm$
fw	1934.92	1934.92
color, habit	black needle	black parallelepiped
crystal system	monoclinic	monoclinic
space group	*C*2/*m*	*C*2/*m*
a, Å	25.3572(10)	25.3389(15)
b, Å	14.9526(6)	14.8092(9)
c, Å	20.5748(8)	20.9260(13)
β, deg	97.439(3)	97.5890(8)
V, Å^3	7735.4(5)	7783.7(8)
Z	4	4
T, K	90(2)	90(2)
radiation (λ, Å)	Mo Kα (0.710 73)	Mo Kα (0.710 73)
unique data	11 714 [*R*(int) = 0.0325]	12 312 [*R*(int) = 0.0390]
parameters	1160	1115
restraints	2877	1277
obsd $I > 2\sigma(I)$ data	9573	10 660
$R1^a$ (obsd data)	0.0662	0.0746
$wR2^b$ (all data)	0.1787	0.1566

^{a}For data with $I > 2\sigma(I)$, $R1 = \sum||F_o| - |F_c||/\sum|F_o|$. ^{b}For all data, $wR2 = \{\sum[w(F_o^2 - F_c^2)^2])/\sum[w(F_o^2)^2]\}^{1/2}$.

The structure of Sm@$D_{3d}(19)$-C_{84}·Ni^{II}(OEP)·2(toluene) shows disorder in its individual components. The asymmetric unit contains a full molecule of $D_{3d}(19)$-C_{84} at a fractional occupancy of 0.5. The molecule is disordered with respect to a crystallographic mirror plane. As a result, two identical fullerene cages reside at a common crystallographic site in mirror-related orientations. In the asymmetric unit there are four samarium sites: a major site with a fractional occupancy of 0.40 and three minor sites with occupancies of 0.05, 0.03, and 0.02. There are two toluene sites near mirror planes. In one of these sites in the asymmetric unit, there are two different orientations of a toluene molecule that have relative occupancies of 0.40/0.10.

The structure of Sm@$C_2(13)$-C_{84}·Ni^{II}(OEP)·2(toluene) shows varying degrees of disorder in the individual components. The asymmetric unit contains two full molecules of $C_2(13)$-C_{84} with refined fractional occupancies of 0.4629(15) and 0.0371(15). These two molecules have different orientations, and both are disordered with respect to a crystallographic mirror plane. In the asymmetric unit

dx.doi.org/10.1021/ja211785u | *J. Am. Chem. Soc.* 2012, 134, 5331−5338

there are 10 samarium sites: a major site with a fractional occupancy of 0.21 and two minor sites with occupancies of 0.05, one with 0.04 occupancy, four with occupancy of 0.03, and two with occupancy of 0.02. There are also two disordered toluene molecules present.

Computational Details. Geometries of the four isomers of Sm@C_{84} were fully optimized by nonlocal density functional calculations at the B3LYP level.[38] The effective core potential and basis set developed by Stevens et al.[39] were used for samarium (CEP-31g), and the split-valence 3-21G basis set was used for carbon. All calculations were carried out with the GAUSSIAN 03 program.[40]

■ ASSOCIATED CONTENT

Supporting Information

Additional text, five figures, and two tables describing synthesis and purification of three Sm@C_{84} isomers, computational details, and complete citation for ref 40 (pdf); and X-ray crystallographic files for Sm@D_{3d}(19)-C_{84}·Ni^{II}(OEP)·2(toluene) (cif) and Sm@C_2(13)-C_{84}·Ni^{II}(OEP)·2(toluene) (cif). This material is available free of charge via the Internet at http://pubs.acs.org.

■ AUTHOR INFORMATION

Corresponding Author

zyliu@zju.edu.cn (Z.L.); mmolmstead@ucdavis.edu (M.M.O.); albalch@ucdavis.edu (A.L.B.)

Author Contributions

‡These authors contributed equally to this work.

Notes

The authors declare no competing financial interest.

■ ACKNOWLEDGMENTS

We thank the U.S. National Science Foundation (Grants CHE-1011760 and CHE-0716843 to A.L.B. and M.M.O.), the National Natural Science Foundation of China (20971108 to Z.L., 11179039 to H.Y., and 10979001, 51025206 to B.L.), and the National Basic Research Program of China (2011CB808200 to B.L.) for support.

■ REFERENCES

(1) Heath, J. R.; O'Brien, S. C.; Zhang, Q.; Liu, Y.; Curl, R. F.; Kroto, H. W.; Tittel, F. K.; Smalley, R. E. *J. Am. Chem. Soc.* **1985**, *107*, 1179–1180.

(2) Lu, X.; Akasaka, T.; Nagase, S. *Chem. Commun.* **2011**, *47*, 5942–5957.

(3) Chaur, M. N.; Melin, F.; Ortiz, A. L.; Echegoyen, L. *Angew. Chem., Int. Ed.* **2009**, *48*, 7514–7538.

(4) Komatsu, K.; Murata, M.; Murata, Y. *Science* **2005**, *307*, 238–240.

(5) (a) Kurotobi, K.; Murata, Y. *Science* **2011**, *333*, 613–616. (b) Balch, A. L. *Science* **2011**, *333*, 531–532.

(6) (a) Stevenson, S.; Mackey, M. A.; Stuart, M. A.; Philips, J. P.; Easterling, M. L.; Chancellor, C. J.; Olmstead, M. M.; Balch, A. L. *J. Am. Chem. Soc.* **2008**, *130*, 11844–11845. (b) Mercado, B. Q.; Olmstead, M. M.; Beavers, C. M.; Easterling, M. L.; Stevenson, S.; Mackey, M. A.; Coumbe, C. E.; Phillips, J. D.; Phillips, J. P.; Poblet, J. M.; Balch, A. L. *Chem. Commun.* **2010**, *46*, 279–281.

(7) Mikawa, M.; Kato, H.; Okumura, M.; Narazaki, M.; Kanazawa, Y.; Miwa, N.; Shinohara, H. *Bioconjugate Chem.* **2001**, *12*, 510–514.

(8) Bolskar, R. D.; Benedetto, A. F.; Husebo, L. O.; Price, R. E.; Jackson, E. F.; Wallace, S.; Wilson, L. J.; Alford, J. M. *J. Am. Chem. Soc.* **2003**, *125*, 5471–5478.

(9) Shultz, M. D.; Duchamp, J. C.; Wilson, J. D.; Shu, C.-Y.; Ge, J.; Zhang, J.; Gibson, H. W.; Fillmore, H. L.; Hirsch, J. I.; Dorn, H. C.; Fatouros, P. P. *J. Am. Chem. Soc.* **2010**, *132*, 4980–4981.

(10) Rodríguez-Fortea, A.; Balch, A. L; Poblet, J. M. *Chem. Soc. Rev.* **2011**, *40*, 3551–3563.

(11) Rodriguez-Fortea, A.; Alegret, N.; Balch, A. L.; Poblet, J. M. *Nat. Chem.* **2010**, *2*, 955–961.

(12) (a) Okazaki, T.; Lian, Y. F.; Gu, Z. N.; Suenaga, K.; Shinohara, H. *Chem. Phys. Lett.* **2000**, *320*, 435–440. (b) Lian, Y.; Shi, Z.; Zhou, X.; He, X.; Gu, Z. *Chem. Mater.* **2001**, *13*, 39–42.

(13) Liu, J.; Shi, Z. J.; Gu, Z. N. *Chem.—Asian J.* **2009**, *4*, 1703–1711.

(14) Okazaki, T.; Suenaga, K.; Lian, Y.; Gu, Z.; Shinohara, H. *J. Chem. Phys.* **2000**, *113*, 9593–9597.

(15) Okazaki, T.; Suenaga, K.; Lian, Y.; Gu, Z.; Shinohara, H. *J. Mol. Graphics Modelling* **2001**, *19*, 244–251.

(16) Yang, H.; Jin, H. X.; Zhen, H.; Wang, Z. M.; Liu, Z. L.; Beavers, C. M.; Mercado, B. Q.; Olmstead, M. M.; Balch, A. L. *J. Am. Chem. Soc.* **2011**, *133*, 6299–6306.

(17) Stone, A. J.; Wales, D. J. *Chem. Phys. Lett.* **1986**, *128*, 501–503.

(18) Fowler, P. W.; Manolopoulous, D. E. *An Atlas of Fullerenes*; Clarendon: Oxford, U.K., 1995.

(19) Kikuchi, K.; Nakahara, N.; Wakabayashi, T.; Suzuki, S.; Shinohara, H.; Miyake, Y.; Saito, K.; Ikemoto, I.; Kainosho, M.; Achiba, Y. *Nature* **1992**, *357*, 142–145.

(20) Dennis, T. J. S.; Kai, T.; Asato, K.; Tomiyama, T.; Shinohara, H.; Yoshida, T.; Kobayashi, Y.; Ishiwatari, H.; Miyake, Y.; Kikuchi, K.; Achiba, Y. *J. Phys. Chem. A* **1999**, *103*, 8747–8751.

(21) Tagmatarchis, N.; Avent, A. G.; Prassides, K.; Dennis, T. J. S.; Shinohara, H. *Chem. Commun.* **1999**, 1023–1024.

(22) Tagmatarchis, N.; Okada, K.; Tomiyama, T.; Yoshida, T.; Kobayashi, Y.; Shinohara, H. *Chem. Commun.* **2001**, 1366–1367.

(23) Balch, A. L.; Ginwalla, A. S.; Lee, J. W.; Noll, B. C.; Olmstead, M. M. *J. Am. Chem. Soc.* **1994**, *116*, 2227–2228.

(24) Epple, L.; Amsharov, K.; Simeonov, K.; Dix, I.; Jansen, M. *Chem. Commun.* **2008**, 5610–5612.

(25) Kareev, I. E.; Kuvychko, I. V.; Shustova, N. B.; Lebedkin, S. F.; Bubnov, V. P.; Anderson, O. P.; Popov, A. A.; Boltalina, O. V.; Strauss, S. H. *Angew. Chem., Int. Ed.* **2008**, *47*, 6204–6207.

(26) Tamm, N. B.; Sidorov, L. N.; Kemnitz, E.; Troyanov, S. I. *Chem.—Eur. J.* **2009**, *15*, 10486–10492.

(27) Beavers, C. M.; Zuo, T.; Duchamp, J. C.; Harich, K.; Dorn, H. C.; Olmstead, M. M.; Balch, A. L. *J. Am. Chem. Soc.* **2006**, *128*, 11352–11353.

(28) Zuo, T.; Walker, K.; Olmstead, M. M.; Melin, F.; Holloway, B. C.; Echegoyen, L.; Dorn, H. C.; Chaur, M. N.; Chancellor, C. J.; Beavers, C. M.; Balch, A. L.; Athans, A. J. *Chem. Commun.* **2008**, 1067–1069.

(29) Kurihara, H.; Lu, X.; Iiduka, Y.; Nikawa, H.; Hachiya, M.; Mizorogi, N.; Slanina, Z.; Tsuchiya, T.; Nagase, S.; Akasaka, T. *Inorg. Chem.* **2012**, *51*, 746–750.

(30) Sun, D.-Y.; Liu, Z.-Y.; Guo, X.-H.; Xu, W.-G.; Liu, S.-Y. *J. Phys. Chem. B* **1997**, *101*, 3927–3930.

(31) Mercado, B. Q.; Jiang, A.; Yang, H.; Wang, Z.; Jin, H.; Liu, Z.; Olmstead, M. M.; Balch, A. L. *Angew. Chem., Int. Ed.* **2009**, *48*, 9114–9116.

(32) Olmstead, M. M.; Costa, D. A.; Maitra, K.; Noll, B. C.; Phillips, S. L.; Van Calcar, P. M.; Balch, A. L. *J. Am. Chem. Soc.* **1999**, *121*, 7090–7097.

(33) Wang, C.-R.; Kai, T.; Tomiyama, T.; Yoshida, T.; Kobayashi, Y.; Nishibori, E.; Takata, M.; Sakata, M.; Shinohara, H. *Angew. Chem., Int. Ed.* **2001**, *40*, 397–399.

(34) Yamazaki, Y.; Nakajima, K.; Wakahara, T.; Tsuchiya, T.; Ishitsuka, M. O.; Maeda, Y.; Akasaka, T.; Waelchli, M.; Mizorogi, N; Nagase, S. *Angew. Chem., Int. Ed.* **2008**, *47*, 7905–7908.

(35) Xu, Z.; Nakane, T.; Shinohara, H. *J. Am. Chem. Soc.* **1996**, *118*, 11309–11310.

(36) Lu, X.; Slanina, Z.; Akasaka, T.; Tsuchiya, T.; Mizorogi, N.; Nagase, S. *J. Am. Chem. Soc.* **2010**, *132*, 5896–5905.

(37) Sheldrick, G. M. *Acta Crystallogr.* **2008**, *A64*, 112–122.

(38) (a) Becke, A. D. *Phys. Rev. A* **1988**, *38*, 3098–3100. (b) Lee, C.; Yang, W.; Parr, R. G. *Phys. Rev. B* **1988**, *37*, 785–789.

(39) Stevens, W.; Basch, H.; Krauss, J. *J. Chem. Phys.* **1984**, *81*, 6026–6033.

(40) Frisch, M. J. et al., Gaussian 03, Revision C.02.
(41) Xu, J. X.; Lu, X.; Zhou, X. H.; He, X. R.; Shi, Z. J.; Gu, Z. N. *Chem. Mater.* **2004**, *16*, 2959−2964.